PHYSICAL MODELING OF BASE CARRIER LIFETIME AND FREQUENCY RESPONSE OF HETEROJUNCTION BIPOLAR TRANSISTOR

BY

YUE LI

THESIS

Submitted in partial fulfillment of the requirements
for the degree of Master of Science in Electrical and Computer Engineering
in the Graduate College of the
University of Illinois at Urbana-Champaign, 2019

Urbana, Illinois

Adviser:

Professor Jean-Pierre Leburton

Abstract

Based on the observation of the degradation of the base transfer factor caused by the insertion of the quantum well (QW) together with the heavy base doping, this work demonstrates the physical modeling of the quantum-well heterojunction bipolar transistor, known as the transistor laser. By revising the conventional bipolar junction transistor charge control model, this work accounts for the degraded base transfer ratio, which contrasts with the constant base transport factor close to unity in conventional bipolar junction transistor operation, and its variation with the base current. The approach of this work is to assess the concentration of base minority carrier captured in the QW and give an analytical expression for the carrier lifetime in the base, which is a key factor for device frequency performance. Expressions for the physical parameters such as capture time, base recombination lifetime and base transit time are obtained in terms of experimental values such as base current, and device design parameters such as base width, QW width and QW location. While the calculated base recombination lifetime can be of the order of a fraction of a nanosecond, the QW capture time is found to be of the order of a picosecond. These parameters retrieved from the calculation are then used to successfully reproduce the optical frequency response diagrams of the light-emitting transistor and transistor laser obtained from experiments.

Acknowledgments

Many thanks to Professor Jean-Pierre Leburton for his caring support and kind guidance throughout my bachelor's and master's journey. Thanks to Nagendra, Mingye and Bohao for their constant support and help during the two years we spent in MNTL. Finally, thanks to my family and all my friends for their love and support. This work is sponsored in part by E2CDA-NRI, a funded center of NRI, a Semiconductor Research Corporation (SRC) program sponsored by NERC and NIST under Grant No. NERC 2016-NE-2697-A, and by the National Science Foundation under Grant No. ECCS 16-40196.

Contents

1. Introduction

Semiconductor light-emitting devices are used widely in optoelectronic applications such as optical-fiber communication, video recording and high-speed laser printing due to their portable size, low power consumption, and their ability to modulate the output by adjusting the injection current. The quantum-well (QW) heterojunction bipolar transistor (HBT) is a type of semiconductor laser comprised of layers of direct bandgap n-InGaP/p+-GaAs/n-GaAs materials configured as a traditional bipolar junction transistor (BJT) with a set of intrinsic InGaAs QWs with smaller bandgap than the bulk base inserted in the heavily doped base region. The QWs are usually placed near the collector end of the base to intercept electrons injected from the emitter for radiative recombination with the holes, before they rush to the collector. The common BJTs, usually with heavy emitter doping and light base doping, suppress base recombination since maximum preservation of current from emitter to collector is desired. However, for QW-HBT, carrier recombination is enhanced for lasing purpose due to the presence of smaller bandgap QWs in the base region which capture and confine the carrier. The base recombination and base current take an important role in transistor operation not only in separating the high-impedance collector from the low-impedance emitter, but also in modulating optical output. The suppression of base transport factor caused by the heavy base doping as well as the insertion of the QW, and its variation with the base current, are observed and analyzed in this work to characterize the behavior of the QW-HBT.

2. Literature Review

The quantum well (QW) heterojunction bipolar transistor (HBT), known as the transistor laser (TL), is a three-port optoelectronic device modified based on conventional bipolar junction transistor (BJT) by adding layers of intrinsic materials in the heavily doped base as QWs to collect carriers, thus enhancing recombination. Ever since its invention by Then, Feng and Holonyak, the QW-HBT has been intensively investigated both experimentally [1]–[4] and theoretically [5]–[10]. Inserted in the heavily doped base, the QW serves as an optical "collector" that captures the carriers injected from the emitter to the base, giving the QW-HBT an optical output in addition to the traditional collector which produces electrical output. This enables photon storage and switching and the modulation of optical output by controlling the base current [11], [12]. The QW-HBT integrates the advantages of both a laser and a transistor, making it possible to achieve high-frequency response without sharp resonance which enables compact and fast optoelectronic such as frequency multiplication [13], [14], nonlinear signal mixing [15] and negative resistance [16]. By modifying the QW-HBT design, one can modulate electrical and optical properties since the base QW governs the charge recombination in the base [17], [18], and hence enables the tailoring of the optical and electrical properties, improving error-free data transmission to as high as 22 Gb/s [11], [19-21].

Due to the presence of the QW in the base that enhances carrier capture and recombination, the traditionally triangular base minority carrier profile becomes broken at the center of the QW, which induces the degradation of the current transfer ratio ($\alpha = \Delta I_C / \Delta I_E$), normally ~ 1 in traditional BJTs. Because of this fast QW capture process, the conventionally triangular minority charge profile in the transistor base now becomes broken at the center of the QW (Fig. 1). This broken carrier profile significantly degrades the current transfer ratio ($\alpha = \Delta I_C / \Delta I_E$), normally close to unity in conventional bipolar junction transistors.

Furthermore, experimental data shows a linear relation between the base current I_B and α [19], [22]. This suppressed electronic gain due to enhanced QW recombination rate revealed a strong correlation with the photonic operation and electronic characteristics of the QW-HBT.

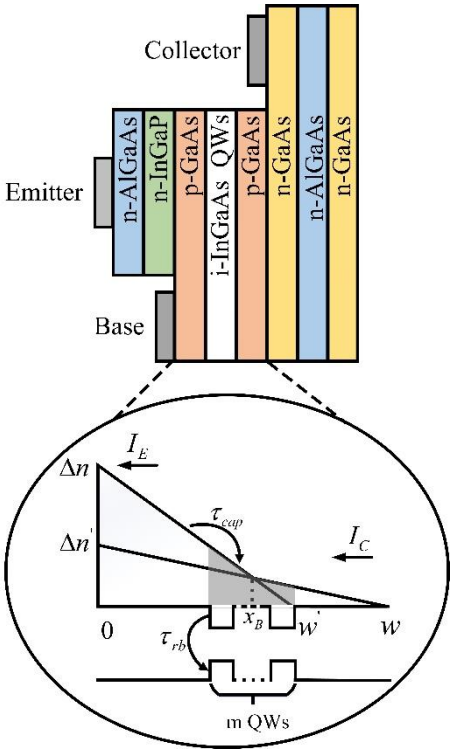

Figure 1. Schematic of the layered HBLET structure (upper diagram) with the minority carrier profile (lower diagram) in the transistor base caused by the QW capture. The emitter and the collector are on the left and right side of the base, respectively. The shaded area in the lower diagram indicates the minority carrier concentration above the m-QWs. w and x_B denote the base width and the middle point of QW location, respectively.

This work utilizes the Z-L rate equation which complements the traditional coupled photon-carrier rate equations that are used to describe the radiative emission in laser diode [7]. The Z-L equation takes into account the slow recombination in the bulk of the base as well as the quick carrier capture process in the QW of the base. These carrier dynamics in the base are related by a geometry factor ν which represents the percentage of base carriers above the QW that can be captured for fast radiative recombination (see Fig. 1). Premised on the Z-L rate equation, this work develops a charge control analysis on the basis of the empirical expression for ν, which relates various time constants such as the base transit time (τ_{tr}), the

QW capture time (τ_{cap}) and the base minority carrier lifetime (τ_b) to α. In particular, this work shows that τ_b can be determined from the injection current and the device design parameters through their common dependence on α.

3. Theory and Model

Composed of layers of direct bandgap III-V materials structured as a n-p+-n BJT, the QW-HBTs studied in this work has one or several intrinsic QW(s) (i-InGaAs) placed in the base region [23]–[25]. The QW(s), usually inserted near the collector end of the heavily p-doped base, capture(s) the electrons for radiative recombination with the holes when they are injected from the emitter to collector, resulting in a drop in the minority carrier concentration profile along the base (see Fig. 1).

As such, two processes compose the carrier lifetime in the base, 1) direct radiative recombination in the base outside the QW(s) and 2) the carrier capture in the vicinity of the QW that causes the direct recombination of the electrons with the holes. The two processes can be described in Eqn. (4) below, which complements the normal coupled carrier-photon rate equation.

$$\frac{dn(t)}{dt} = \frac{\nu Q_b(t)}{q\tau_{cap}} - \frac{n(t)}{\tau_{qw}} - \Omega\left[n(t) - n_{nom}\right]N_p(t) \tag{1}$$

$$\frac{dN_p(t)}{dt} = \Omega\left[n(t) - n_{nom}\right]N_p(t) + \frac{\theta n(t)}{\tau_{qw}} - \frac{N_p(t)}{\tau_p} \tag{2}$$

$$\frac{dQ_b(t)}{dt} = J_B(t) - \frac{Q_b(t)}{\tau_b} \tag{3}$$

$$\frac{1}{\tau_b} = \frac{\nu}{\tau_{cap}} + \frac{1-\nu}{\tau_{b0}} \approx \frac{\nu}{\tau_{cap}} \tag{4}$$

Eqn. (1) characterizes the rate of change for base carriers in the QW, where $n(t)$ denotes the QW carrier density, q and Q_b are the electron charge and the base charge density, respectively. The term τ_{cap} is the QW capture time, and the parameter ν accounts for the fraction of charge above the QW region. Thus, $\nu Q_b(t)/\tau_{cap}$ accounts for the base charge captured by the QW, whereas τ_{qw} is the QW spontaneous recombination lifetime and $n(t)/\tau_{qw}$ characterizes the spontaneous recombination rate. The term n_{nom} represents the transparency carrier density to reach lasing threshold. Ω is the differential gain factor and the stimulate emission lifetime is given by $\tau_{st} = \left[\Omega N_p(t)\right]^{-1}$, where $N_p(t)$ is the photon density. The photon dynamics are characterized in Eqn. (2), which includes photon decay and both stimulated and

spontaneous recombination. The first term in Eqn. (2) represents the number of photons generated in the stimulated emission starting after the carrier density surpassed the transparency carrier density. In the second term, $N_p(t)/\tau_p$ accounts for the photon loss rate, where τ_p is the photon lifetime and the θ represents the fraction of spontaneous emission coupled to the cavity mode (a very small number, since there are thousands of modes possible for spontaneous emission, but only one mode would dominate in the stimulated emission). Eqn. (3) characterizes all of the carriers in the base, in which the first term $J_B(t)$ is the base current density and the second term accounts for the loss of carriers in the base due to both QW capture and recombination happening in the bulk of the base. The physical quantities and parameters used in the model and the derivation are summarized in Table 1 at the end of this chapter.

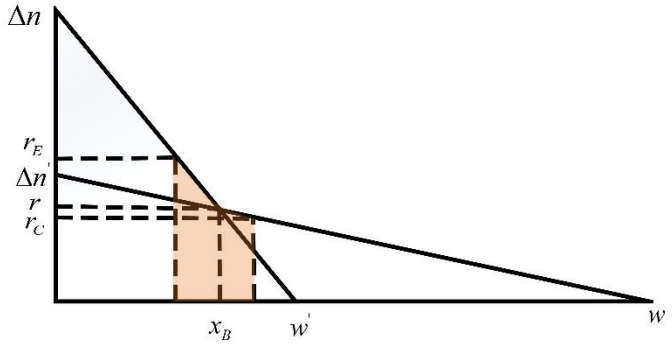

Figure 2. Detailed illustration of base carrier profile. The shaded area represents the QW region.

Operating in forward biased mode, electrons rapidly cross the base and undergo limited loss through recombination when injected from the emitter, except for those electrons captured by the QW, where they stay before recombination by spontaneous or stimulated emission. The QW capture in the base region causes the base current density to drop substantially. This attribute is approximated by a slope change in the carrier concentration profile illustrated in Fig. 2.

Hence, the minority charge density in the base region can be calculated from the two overlapping triangles shown in Fig. 2 as $q\Delta nAw'/2$ and $q\Delta n'Aw/2$, where Δn is the maximum minority carrier concentration at the emitter side and w is the base width. The terms $\Delta n'$ and w' are their reduced values

caused by the QWs, respectively. From triangle property, $w' = \alpha w + (1-\alpha)x_B$ and $\Delta n' = \Delta n \alpha w / [\alpha w + (1-\alpha)x_B]$. In the diffusion approximation of the BJT charge control analysis [26], the emitter current I_E and collector current I_C can be expressed as:

$$I_E = qAD_n \frac{d\delta n_E}{dx_E} = qAD_n \frac{\Delta n}{w'} = qD_n \frac{\Delta n}{\alpha w + (1-\alpha)x_B} \tag{5}$$

$$I_C = qAD_n \frac{d\delta n_C}{dx_C} = qAD_n \frac{\Delta n'}{w} = qD_n \frac{\alpha \Delta n}{\alpha w + (1-\alpha)x_B} \tag{6}$$

Since the base transport factor $\alpha = I_C / I_E = \Delta n' w' / \Delta n w$, the base current can be derived:

$$I_B = I_E - I_C = \frac{qAD_n(1-\alpha)}{\alpha w + (1-\alpha)x_B} \Delta n \tag{7}$$

From triangle geometry one can calculate the intermediate parameters $r = \Delta n \alpha (w - x_B) / [\alpha(w - x_B) + x_B]$, $r_E = \Delta n \left[\alpha (w - x_B) + \frac{w_{qw}}{2} \right] \Big/ [\alpha(w - w_B) + x_B]$ and $r_C = \Delta n \alpha \left(w - x_B - \frac{w_{qw}}{2} \right) \Big/ [\alpha(w - x_B) + x_B]$, which can then be used in calculating the area of the two trapezoids in the shadowed region.

From the parameters derived above, and from the quasi-linear carrier concentration profile, one can express the base charge above the QWs n_{qw} and the total base carrier density n_b as a function of the minority carrier concentration Δn, total QW width w_{qw}, QW center location x_B, base width w and the current transfer ratio α:

$$n_b = \frac{\alpha w^2 + (1-\alpha)x_B^2}{2[\alpha w + (1-\alpha)x_B]} \Delta n \tag{8}$$

$$n_{qw} = w_{qw} \frac{\alpha(w - x_B) + \frac{1}{8} w_{qw}(1-\alpha)}{\alpha w + (1-\alpha)x_B} \Delta n \tag{9}$$

The presence of the m-QWs is approximated as one single QW centered at x_B, where the carrier concentration slope changes. To account for the multiple QWs in the base, the total QW width is given by

$w_{qw} = m \cdot w_{sqw} + (m-1) \cdot d_{qw}$, where w_{sqw} denotes the width of a single QW, m is the QW number and d_{qw} represents the spacing between the QWs. The geometry factor ν given by the ratio of n_{qw} and n_b is defined as the fraction of the base charge above the QW.

$$\nu = \frac{n_{qw}}{n_b} = \frac{8\alpha w_{qw}(w - x_B) + (1-\alpha) w_{qw}^2}{4\left[\alpha w^2 + (1-\alpha) x_B^2\right]} \tag{10}$$

The bulk carrier lifetime is orders of magnitude larger than the carrier lifetimes in the QW, despite the fact that the heavy p-doping in the base enhances recombination rate, causing the minority carrier lifetime to be much shorter than those in conventional diode lasers.

The emitter current efficiency can be approximated to be unity $\gamma = 1$ due to the large hetero-barrier at the emitter-base junction. If one assumes negligible base recombination outside the QW when no stimulated emission occurs (DC condition), the spontaneous recombination current in the undoped QW can be approximate as the total base current I_B, i.e. $I_B / qA = n / \tau_{qw}$, where A is the junction area. Thus, from Eqn. (1), one can obtain the steady state equation:

$$\frac{\nu n_b}{\tau_{cap}} = \frac{n}{\tau_{qw}} = \frac{I_B}{qA} \tag{11}$$

In these conditions, one can approximate the collector current amplification factor by τ_{tr}, the average time for excess electrons to transit from the emitter to the collector and τ_b, the minority carrier lifetime in the base as $\beta = i_C / i_B = \tau_b / \tau_{tr}$. From Eqns. (6) and (8), the expressions for τ_{tr} and τ_b are as follows:

$$\tau_{tr} = \frac{qAn_b}{I_C} = \frac{\alpha w^2 + (1-\alpha) x_B^2}{2D_n \alpha} \tag{12}$$

$$\tau_b = \beta \tau_{tr} = \frac{qAn_b}{I_B} = \frac{\alpha w^2 + (1-\alpha) x_B^2}{2D_n (1-\alpha)} \tag{13}$$

Here, the base carrier lifetime $\tau_b = 1 / \left[\nu / \tau_{cap} + (1-\nu) / \tau_{rb0}\right]$ is the weighted sum of QW capture ν / τ_{cap} and the base recombination occurring outside the QW $(1-\nu) / \tau_{rb0}$. By neglecting the slow recombination

happening in the bulk base, one can assume that most of the recombination takes place in the QW. From there, the base carrier lifetime and the capture time can be expressed by:

$$\tau_{cap} = \nu\tau_b = \frac{w_{qw}\left[\alpha\left(w - x_B\right) + \frac{1}{8}w_{qw}\left(1-\alpha\right)\right]}{D_n\left(1-\alpha\right)} \tag{14}$$

The analytical expression for the geometry factor ν and the carrier lifetimes can then be used to characterize the QW-HBT operation from the design parameters of each device and their correlation with the devices' current transfer ratios.

Table 1. Physical Quantities and Parameters

Symbol	Definition	Unit
t	Time	s
I_E	Emitter current	Amp
I_B	Base current	Amp
I_C	Collector current	Amp
α	Current transfer ratio	-
ν	QW geometry factor	-
β	Collector current amplification factor	-
Ω	Differential gain factor	cm^2s^{-1}
θ	Fraction of spontaneous emission coupled to cavity mode	-
κ	QW expansion factor	-
τ_{cap}	QW electron capture time	s
τ_{qw}	QW spontaneous recombination lifetime	s
τ_{st}	QW stimulated recombination lifetime	s
τ_{tr}	Base transit time	s
τ_b	Base charge lifetime	s
τ_{b0}	Bulk base charge lifetime	s
τ_p	Photon lifetime	s
n	QW electron density, to be recombined	cm^{-2}
n_0	Steady state QW electron density	cm^{-2}
δn	QW electron density response to AC current component	cm^{-2}
n_{nom}	Transparency electron density	cm^{-2}
n_{qw}	Base electron density above QW, to be captured	cm^{-2}
n_b	Total base charge density	cm^{-2}
N_p	Photon density	cm^{-2}

Table 1. Continued

N_{p0}	Steady state photon density	cm^{-2}
δN_p	Photon density response to AC current component	cm^{-2}
Q_b	Base charge density	$Coulomb \cdot cm^{-2}$
Q_{b0}	Steady state base charge density	$Coulomb \cdot cm^{-2}$
δQ_b	Base charge density response to AC current component	$Coulomb \cdot cm^{-2}$
J_B	Base current density	$Amp \cdot cm^{-2}$
J_{B0}	Steady state base current density	$Amp \cdot cm^{-2}$
δJ_B	Base current density response to AC current component	$Amp \cdot cm^{-2}$
A	Junction area	cm^2

4. Description of Research Results

4.1 Heterojunction Bipolar Light-Emitting Transistor (HBLET)

For the HBLET, recombination is mostly spontaneous recombination; thus, the rate equation is modified from the coupled carrier-photon rate equation from the Z-L model by discarding the term that includes stimulated emission. Fig. 3(a) shows the relationship of the base current I_B and the base transfer ratio α as obtained from and HBLET with 2 QWs in experiment [22]. The degraded α value as compared with normal BJT with no QW insertions is caused by the strong QW capture in the HBLET. As I_B increases, the value of α increases linearly due to high carrier injection, thus more carriers reach the collector.

The density of states (DOS) of the carriers in the QW becomes two-dimensional (2D) because the injected electrons and holes are quantized only in the direction perpendicular to the active region. The 2D-DOS represents the number of states per unit energy interval near energy level E per unit area in the momentum (n) space of a particle. Each state (n_i) in the momentum space corresponds to one wave oscillation mode (k_i) since $k_i = n_i\pi/L = 2\pi/\lambda_i$, where L is the QW width. The number of normal modes in the first quadrant (since n_i are positive integers) of n-space is $N^{'} = \pi n^2/4$, where $n = kL/\pi = L\sqrt{2mE}/(\pi\hbar)$, m is electron mass and $\hbar$ is reduced Planck constant. Including two possible spins, $N = \pi n^2/2 = mL^2E/\pi\hbar^2$. Then, by taking the derivatives $dN/dE = mE/\pi\hbar^2$, one can find the number of electron states within an energy interval dE, between E and $E + dE$. From there, the number of states per unit energy interval near E per unit volume can be readily expressed as $D(E) = dN/dE \cdot 1/L^2 = m/\pi\hbar^2$. Putting the 2D DOS equation as well as the Fermi distribution $f(E) = \left\{\exp\left[(E_0 - E_F)\right]/kT + 1\right\}^{-1}$ together, one can find the QW 2D carrier density $n_{qw} = \int_{E_0}^{E_{Fn}} D(E)\, f(E)\, dE = m^* kT/\pi\hbar^2 \cdot \ln\left\{1 + \exp\left[(E_{Fn} - E_0)/kT\right]\right\}$, where $m^*/\pi\hbar^2$ is the 2D density of state, k is the Boltzmann constant, E_{Fn} is the quasi-Fermi level and

E_0 is the ground state level. In this work, the temperature T = 300 K and effective mass $m^* = 0.057m_0$ for $In_{0.15}Ga_{0.85}As$, where m_0 is the free electron mass.

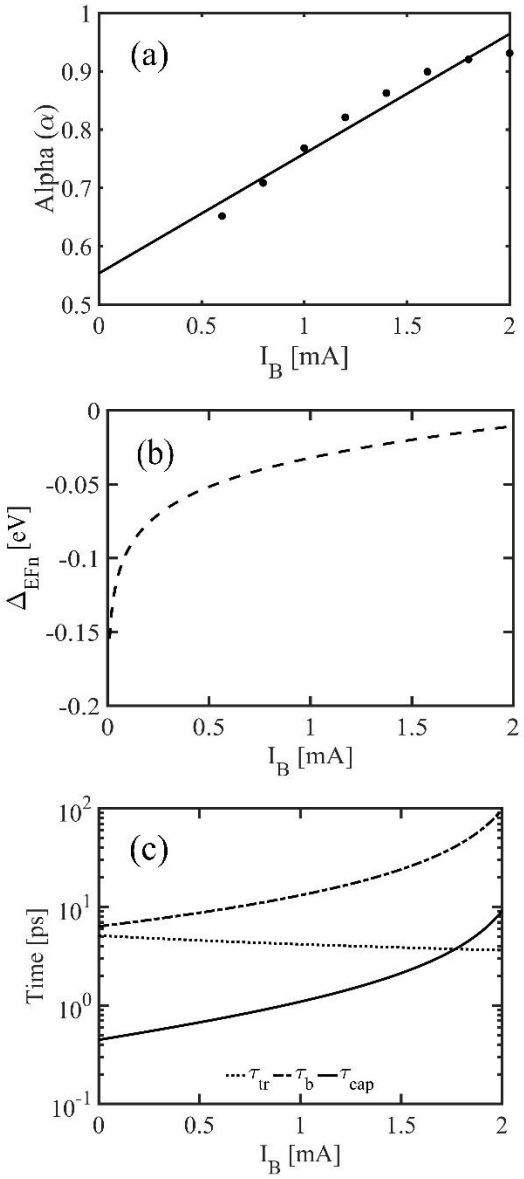

Figure 3. (a) Dependence of current transport factor α on the base current I_B in the HBLET consisting of 2 QWs (m=2) in the base of Ref [22]. The experimental data are represented as the dots. **(b)** Quasi-Fermi level with respect to the ground level ΔE_{Fn} as a function of I_B. **(c)** Capture time τ_{cap} (solid curve), transit time τ_{tr} (dotted curve) and base lifetime τ_b (dashed curve) as a function of base current I_B for HBLET.

Rearranging the 2D carrier density equation and Eqns. (7) and (9) from the manuscript, one can get $\Delta E_F = E_{Fn} - E_0 = kT \ln\left[\exp\left(\pi\hbar^2 n_{qw}/m^* kT\right) - 1\right]$ and

$n_{qw} = \left\{w_{qw}\left[\alpha\left(w - x_B\right) + w_{qw}\left(1-\alpha\right)/8\right]I_B\right\}/\left[qAD_n\left(1-\alpha\left(I_B\right)\right)\right]$ where α is a function of I_B (plotted in Fig. 3(b)).

From the expression, one can deduce that the E_{Fn} level would also get closer to the ground level E_0 as injection level increases. For the valance band in the InGaAs QW region, because of the space charge effect in the heavily doped base, it would almost line up with the valance band in the GaAs bulk base region. Thus, one can approximate the $In_{0.15}Ga_{0.85}As - GaAs$ bandgap difference ΔE_g ~ 150 meV as the QW depth in the conduction band. As the ground state E_0 in the QW conduction band is estimated to be 120 meV below the conduction band edge of the GaAs base, i.e. about 30 meV above the InGaAs conduction band bottom, from Fig. 3(b), at I_B = 1.6 mA, E_{Fn} is 15 meV below E_0 and 135 meV below the conduction band edge of the GaAs bulk base region. This bandgap profile results in a concentration of about 2.5×10^{17} cm^{-3}. Thus, as calculated with the Fermi-Dirac statistics, the thermally excited carriers in the GaAs base region around the QW reach a concentration of about 2.5×10^{15} cm^{-3}.

From Fig. 3(a), when I_B = 1.6 mA, I_E and α correspond to the value of 16 mA and 0.9, respectively. From Eqn. (5) one can calculate that at the emitter-base junction $\Delta n = 4\times10^{15}$ cm^{-3}. This shows a current overflow across the base, which explains electron accumulation in the QW that causes the enhancement of α and τ_{cap} (shown in Fig. 3(c)).

The time constants τ_{cap}, τ_{tr}, τ_b for the same HBLET structure ($m = 2$, x_B = 75 nm, w_{sqw} = 112 Å, d_{qw} = 20 Å [23] and $\kappa = 1$) are then used to extract the $\alpha - I_B$ relation are shown in Fig. 3(c) as a function of I_B. With increasing base carrier injection, the base lifetime τ_b is incremented from 6.5 ps to 100 ps. The transit time τ_{tr} calculated from our model decreases from 5 ps to 3.8 ps as base current rises from 0 mA to

2 mA, whereas for conventional GaAs BJT with base width $w_B =$ 140 nm at the steady state excess carrier injection condition, the carrier transit time is $w_B^2/2D_n \sim 3.75$ ps ($D_n = 26$ cm^{2}s^{-1} [27]). The discrepancy between the HBLET and the conventional BJT transit time is due to the presence of the QWs in the base region of the HBLET which induces carrier capture process and thus extends the carrier transit process. While the carrier transit time shortens from 5 ps to 3.8 ps, the QW carrier capture time τ_{cap} increases from 0.45 ps to 9 ps with increasing I_B.

By solving rate equations for small sinusoidal signal superimposed to the DC current, one can obtain the optical frequency response for a HBLET. The normalized small signal frequency response can be expressed as:

$$\frac{\delta N_p(\omega)}{\delta J_B(\omega)} = \frac{1}{1+j\omega\tau_b}\frac{1}{1+j\omega\tau_{qw}}\frac{1}{1+j\omega\tau_p} \tag{15}$$

Here τ_b (Fig. 3(c)) is obtained from its relationship to $\alpha(I_B)$ as interpolated from Fig. 3(a).

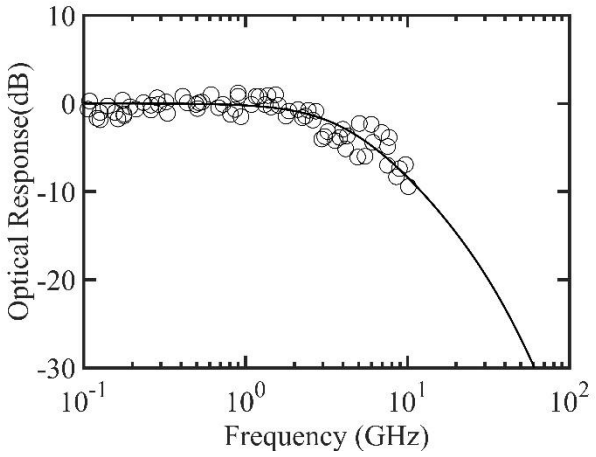

Figure 4. Small signal frequency response of the LET. The -3 dB frequency falls at ~4 GHz. The experimental data [22] are represented in dots.

Assuming a photon lifetime of $\tau_p =$ 2 ps and an effective recombination lifetime τ_{qw} of ~ 37 ps, which accounts for the 2.5 times bandwidth improvement of the HBLET from LED [22], Fig. 4 shows the

comparison between the experimental data and the simulation result on a HBLET device with the QW dimensions mentioned above (with device area of $\sim 400 \times 3.7$ μm).

4.2 Heterojunction Bipolar Transistor Laser (HBTL)

During the transit from emitter to collector, the electrons captured by the QW in the base recombine with the holes radiatively in the active region of the HBTL. In scenarios with larger injection where the injected carrier density is orders of magnitude larger than the equilibrium density, a population inversion would be incurred in the active region, where the stimulated emission dominates the absorption of photons, creating optical gain for the device. With the optical gain in the active region, a large amount of injection current is lost due to the high stimulated recombination emission rate in the base QW region, incurring the degradation of the base transfer ratio and the compression in the collector I-V characteristics (Fig. 5(a) [1,3]). Taking into account the base transfer ratio, the base carrier lifetimes for the HBTL graphed according to Eqn. (12), (13) and (14) derived previously are shown in Fig. 5(b). The carrier transit time degrades from 15.1 ps to 5.68 ps and the base carrier lifetime increases from 2.53 ps to 5.17 ps while the base current rises from 0 mA to 100 mA. The carrier capture time $\tau_{cap} = \nu\tau_b$ nearly quadrupled from 0.085 ps to 0.33 ps, since the geometry factor ν almost doubles from 0.034 to 0.065 with increasing base current.

The small signal frequency response equation derived from the Z-L model then utilizes the base carrier lifetime τ_b derived from its dependence on $\alpha(I_B)$ in Eqn. (12) to model the HBTL optical frequency gain. In an edge-emitting laser, the number of available modes is around 10^6 cm^{-3}, thus the term $\theta n/\tau_{qw}$ in the rate equations can be ignored since the fraction of spontaneous emission modes that can be coupled to the cavity mode is negligible. From there, the Z-L model derived from Eqns. (1), (2) and (3) by performing the same phasor analysis as in the HBLET reads the HBTL frequency response as:

$$\frac{\delta N_p(\omega)}{\delta J_B(\omega)} = \left(\frac{1}{1+i\omega\tau_b}\right)\frac{A}{\omega_r^2 - \omega^2 + i\omega\gamma} \tag{16}$$

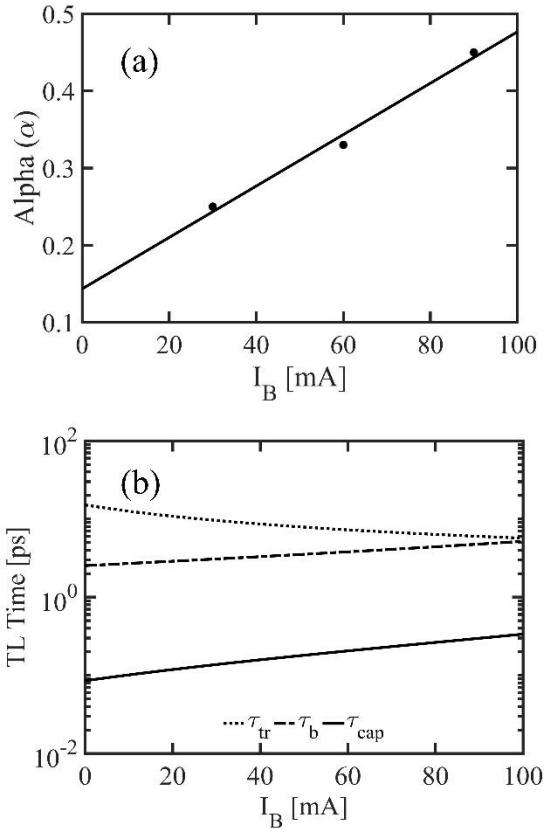

Figure 5. (a) Dependence of current transport factor α on the base current I_B in the HBTL with one QW (m=1) in the base of Ref [3]. The experimental data are represented as the dots. **(b)** Capture time τ_{cap} (solid curve) , transit time τ_{tr} (dotted curve) and base lifetime τ_b (dashed curve) as a function of base current I_B for HBTL.

In Eqn. (16), $A = \Omega \nu N_{p0} \tau_b / q\tau_{cap} \approx \Omega N_{p0} / q$ by ignoring bulk carrier recombination. The term $\omega_r^2 = \Omega N_{p0} / \tau_p$, and $\gamma = 1/\tau_{qw} + \Omega N_{p0}$ where $N_{p0} = n_0 \tau_p / \tau_{qw} \left(J_0 \tau_{qw} / n_0 q - 1 \right)$ and $n_0 = n_{nom} + 1/\Omega \tau_p$.

The HBTL device modeled in this work has only one QW (m=1) centered 0.075 μm away from the emitter-base junction ($x_B =$ 0.075 μm) in the base region (base width $w_B = 0.098$ μm). In this work , the differential gain factor is $\Omega =$ 3 $cm^2 s^{-1}$, and the transparency carrier density is chosen to be $n_{nom} =$ 10^{10} cm^{-2}. The minority carrier concentration is found to be around one 100^{th} that of the typical carrier inversion population in a laser diode, which is usually at the order of 10^{18} cm^{-3} [28].

The GaAs diffusion constant in the presence of 4×10^{19} cm^{-3} doping is $D_n = 26$ cm^{2}s^{-1}, and the spontaneous recombination lifetime and the photon lifetime used in the model are $\tau_{qw} =$ 50 ps and $\tau_p = 7$ ps, respectively [29]. The rest of the parameters used for the HBTL remain the same as the ones used for the HBLET. The calculated optical response along with the comparison with the experimental data from Ref. (3) is shown in Fig. 6. From Eqn. (16), the turning point (peak) of the frequency response happens at $\left(\omega_r^2 - \gamma^2/2\right)^{1/2} = \left[\Omega N_{p0}/\tau_p - 0.5\cdot\left(1/\tau_{qw} + \Omega N_{p0}\right)^2\right]^{1/2} = \left[\Omega N_{p0}\left(1/\tau_p - 1/\tau_{qw} - \Omega N_{p0}/2\right) - 1/2\tau_{qw}^2\right]^{1/2}$. Since τ_p is several orders of magnitude smaller than τ_{qw}, $\Omega N_{p0}/\tau_p$ would dominate this expression.

Also from Eqn. (16), one can see that the damping of the optical frequency response is influenced by τ_b as well as the damping factor $\gamma = 1/\tau_{qw} + \Omega N_{p0}$. Since the damping and the peak location correlate with each other, one cannot increase the peak location without affecting the damping rate. As such the theoretical curves on Fig. 6 are the best fit for the injection condition and the design parameters for this device and show good agreement with the experimental data.

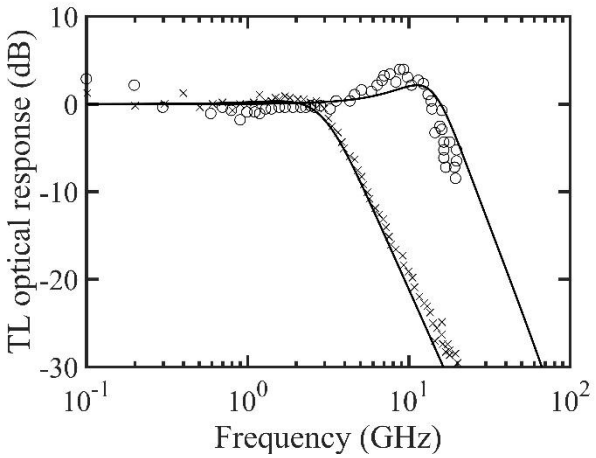

Figure 6. Small signal frequency response for HBTL. The -3 dB frequency falls at ~4 GHz. The left curve represents the frequency response at $I_B =$ 30 mA, $\alpha = 0.25$ and the curve on the right represents frequency response at $I_B =$ 90 mA, $\alpha = 0.45$. The experimental data are represented in dots and crosses.

5. Conclusion

This work reported an analysis of the HBLET and HBTL device carrier dynamics to uncover the relationship among the carrier density, carrier lifetime and the base transfer ratio α. Based on the linear relationship between the transistor base current and the current transfer ratio α, the experimental data and the qualitative theory are related by a charge control analysis to obtain analytical expressions for physical parameters on transistor operation such as the QW capture time τ_{cap}, base recombination lifetime τ_b and base transit time τ_{tr} as a function of α and device design parameters. From the analysis, consistency is achieved between the experimental data of the optical frequency response and the analytical graphs drawn from the theoretical model illustrated in this manuscript.

References

[1] M. Feng, N. Holonyak, and R. Chan, "Quantum-well-base heterojunction bipolar light-emitting transistor," *Appl. Phys. Lett.*, vol. 84, no. 11, pp. 1952–1954, 2004.

[2] M. Feng, J. Qiu, C. Y. Wang, and N. Holonyak, "Tunneling modulation of a quantum-well transistor laser," *J. Appl. Phys.*, vol. 120, p. 204501, 2016.

[3] H. W. Then, M. Feng, and N. Holonyak, "Microwave circuit model of the three-port transistor laser," *J. Appl. Phys.*, vol. 107, p. 094509, 2010.

[4] F. Dixon *et al.*, "Transistor laser with emission wavelength at 1544 nm," *Appl. Phys. Lett.*, vol. 93, p. 021111, 2008.

[5] B. Faraji, D. L. Pulfrey, and L. Chrostowski, "Small-signal modeling of the transistor laser including the quantum capture and escape lifetimes," *Appl. Phys. Lett.*, vol. 93, p. 103509, 2008.

[6] B. Faraji, W. Shi, D. L. Pulfrey and L. Chrostowski, "Analytical modelling of the transistor laser," *IEEE J. Sel. Top. Quantum Electron.*, vol. 15, no. 3, p. 594, 2009.

[7] L. Zhang and J.-P. Leburton, "Modeling of the transient characteristics of heterojunction bipolar transistor lasers," *IEEE J. Quantum Electron.*, vol. 45, no. 4, pp. 359–366, 2009.

[8] I. Taghavi, H. Kaatuzian, and J. P. Leburton, "Bandwidth enhancement and optical performances of multiple quantum well transistor lasers," *Appl. Phys. Lett.*, vol. 100, p. 231114, 2012.

[9] I. Taghavi, H. Kaatuzian, and J. Leburton, "Performance optimization of multiple quantum well transistor laser," *IEEE J. Quantum Electron.*, vol. 49, no. 4, pp. 426–435, 2013.

[10] I. Taghavi, H. Kaatuzian, and J. P. Leburton, "A nonlinear gain model for multiple quantum well transistor lasers," *Semicond. Sci. Technol.*, vol. 28, p. 025022, 2013.

[11] H. W. Then, M. Feng, and N. Holonyak, "The transistor laser: Theory and experiment," *Proc. IEEE*, vol. 101, no. 10, pp. 2271–2298, 2013.

[12] M. Feng, N. Holonyak, A. James, K. Cimino, G. Walter, and R. Chan, "Carrier lifetime and modulation bandwidth of a quantum well AlGaAs/InGaP/GaAs/InGaAs transistor laser," *Appl. Phys. Lett.*, vol. 89, p. 113504, 2006.

[13] J. J. Ebers and J. L. Moll, "Large-signal behavior of junction transistors," *Proc. IRE*, vol. 42, no. 12, pp. 1761–1772, 1954.

[14] Y. Taur and T.H. Ning, *Fundamentals of Modern VLSI Devices*, 2nd ed. Cambridge Univ. Press, 2009.

[15] A. James, N. Holonyak, M. Feng, and G. Walter, "Franz – Keldysh photon-assisted voltage-operated switching of a transistor laser," *IEEE Photonics Technol. Lett.*, vol. 19, no. 9, pp. 680–682, 2007.

[16] J. J. Wierer, P. W. Evans, N. Holonyak, and D. A. Kellogg, "Vertical cavity surface emitting lasers utilizing native oxide mirrors and buried tunnel contact junctions," *Appl. Phys. Lett.*, vol. 72, no. 21, pp. 2742–2744, 1998.

[17] E. A. Rezek, N. Holonyak, B. A. Vojak, and G. E. Stillman, "LPE In1−xGaxP1−zAsz (x 0.12, z 0.26) DH laser with multiple thin-layer (<500 Å) active region," *Appl. Phys. Lett.*, vol. 31, no. 4, p. 288, 1977.

[18] R. D. Dupuis and P. D. Dapkus, N. Holonyak, E. A. Rezek and R. Chin, "Room-temperature laser operation of quantum-well Ga (1 _ x) AlxAs-GaAs laser diodes grown by metalorganic chemical vapor depositional," *Appl. Phys. Lett.*, vol. 32, no. 5, pp. 295–297, 1978.

[19] M. Feng, H. W. Then, N. Holonyak, G. Walter, and A. James, "Resonance-free frequency response of a semiconductor laser," *Appl. Phys. Lett.*, vol. 95, p. 033509, 2009.

[20] C. L. Tang, H. Statz and G. Demars, "Spectral output and spiking behavior of solid-state lasers," *J. Appl. Phys.*, vol. 34, no. 8, pp. 2289–2295, 1963.

[21] Y. Li and J.-P. Leburton, "Quantum well capture and base carrier lifetime in light emitting transistor," *Appl. Phys. Lett.*, vol. 113, p. 171110, 2018.

[22] G. Walter, C. H. Wu, H. W. Then, M. Feng, and N. Holonyak, "Tilted-charge high speed (7 GHz) light emitting diode," *Appl. Phys. Lett.*, vol. 94, p. 231125, 2009.

[23] H. Wang, P. Chou, and C. Wu, "Microwave determination of quantum-well capture and escape time in light-emitting transistors," *IEEE Trans. Electron Devices*, vol. 60, no. 3, pp. 1088–1091, 2013.

[24] H. Wang, S. Member, H. Yang, and C. W. Wu, "Quantum well saturation effect on the reduction of base transit time in light-emitting transistors," *IEEE Trans. Electron Devices*, vol. 61, no. 10, pp. 3472–3476, 2014.

[25] G. Walter, N. Holonyak, M. Feng, and R. Chan, "Laser operation of a heterojunction bipolar light-emitting transistor," *Appl. Phys. Lett.*, vol. 85, no. 20, pp. 4768–4770, 2004.

[26] B. G. Streetman and S. Banerjee, *Solid State Electronic Devices*. Prentice Hall, 2005.

[27] M. Sotoodeh, A. H. Khalid and A. A. Rezazadeh, "Empirical low-field mobility model for III-V compounds applicable in device simulation codes," *J. Appl. Phys.*, vol. 87, no. 6, pp. 2890–2900, 2000.

[28] M. Feng, N. Holonyak, H. W. Then, and G. Walter, "Charge control analysis of transistor laser operation," *Appl. Phys. Lett.*, vol. 91, p. 053501, 2007.

[29] Y. Li and J.-P. Leburton, "Base transport factor and frequency response of transistor lasers Base transport factor and frequency response of transistor lasers," *J. Appl. Phys.*, vol. 126, p. 153103, 2019.